This article was downloaded by:
On: *16 January 2011*
Access details: *Access Details: Free Access*
Publisher *Taylor & Francis*
Informa Ltd Registered in England and Wales Registered Number: 1072954 Registered office: Mortimer House, 37-41 Mortimer Street, London W1T 3JH, UK

Journal of Energetic Materials
Publication details, including instructions for authors and subscription information:
http://www.informaworld.com/smpp/title~content=t713770432

A "Micro-vision" of the Physio-Chemical Phenomena Occurring in Nanoparticles of Aluminum

Alba L. Ramaswamy; Pamela Kaste; S. F. Trevino

Online publication date: 24 June 2010

To cite this Article Ramaswamy, Alba L. , Kaste, Pamela and Trevino, S. F.(2004) 'A "Micro-vision" of the Physio-Chemical Phenomena Occurring in Nanoparticles of Aluminum', Journal of Energetic Materials, 22: 1, 1 — 24
To link to this Article: DOI: 10.1080/07370650490438266
URL: http://dx.doi.org/10.1080/07370650490438266

PLEASE SCROLL DOWN FOR ARTICLE

Full terms and conditions of use: http://www.informaworld.com/terms-and-conditions-of-access.pdf

This article may be used for research, teaching and private study purposes. Any substantial or systematic reproduction, re-distribution, re-selling, loan or sub-licensing, systematic supply or distribution in any form to anyone is expressly forbidden.

The publisher does not give any warranty express or implied or make any representation that the contents will be complete or accurate or up to date. The accuracy of any instructions, formulae and drug doses should be independently verified with primary sources. The publisher shall not be liable for any loss, actions, claims, proceedings, demand or costs or damages whatsoever or howsoever caused arising directly or indirectly in connection with or arising out of the use of this material.

Energetic Materials, 21: 1–24, 2004
Copyright © Taylor & Francis Inc.
ISSN: 0737-0652 print
DOI: 10.1080/07370650490438266

Taylor & Francis
Taylor & Francis Group

A "Micro-vision" of the Physio-Chemical Phenomena Occurring in Nanoparticles of Aluminum

ALBA L. RAMASWAMY

ECE Department, University of Maryland, College Park, MD, USA

PAMELA KASTE

Army Research Laboratory, Aberdeen Proving Grounds, MD, USA

S. F. TREVINO

NIST, National Institute of Standards and Technology

Downloaded At: 13:47 16 January 2011

From Prompt Gamma neutron Activation Analysis (PGAA) of nanoparticles of aluminum, impurities of boron, hydrogen, and water were detected in the material. The morphology of the nanoparticles was examined by atomic force microscopy and high-resolution transmission electron microscopy. The smallest (<10–20 nm) particles were found to be crystallographic in shape, becoming very spherical for larger particle sizes. X-ray diffraction data have evidenced a pristine aluminum crystal lattice, with no residual strain and an amorphous alumina or aluminum hydroxide surface, which is typically about 2.5 nm in thickness. PGAA data revealed that 2 times more water, from absorbed humidity, resided on the nanoaluminum surface as compared with standard "flaked" aluminum. This is

Address correspondence to Alba L. Ramaswamy, ECE Dept., University of Maryland, College Park, MD. E-mail: albalal@eng.umd.edu

providing evidence for the fact that the outer oxide surface in the nanoaluminum appears to have a higher porosity than in the standard ''flaked'' material. Finally, electrostatic charge detected on the nanoaluminum is reported and linked with potential ''dust explosions'' to which the nanoaluminum material might be more susceptible.

Keywords: metallized explosive, propellant, pyrotechnics, rocket

Downloaded At: 13:47 16 January 2011

Introduction

Aluminum is a standard metallic fuel ingredient used in solid rocket propellants. However, merely on a heat release basis, the following is the order of volumetric heat release during oxidation from oxygen: boron>beryllium>aluminum> magnesium>lithium. Note that the typical combustion products of ammonium perchlorate–based propellants contain H_2O, CO_2, and CO as the main oxidizing agents and to a lesser extent O_2. Some of the most effective oxidizers are, in the following order, fluorine monoxide, fluorine, trifluorine nitrogen, ozone, and oxygen [2]. The oxidizing agents produced in a propellant and their reactions with the fuel ingredients are thus important. Aluminum has become the most common solid propellant fuel additive, in part due to its higher availability and low cost.

Aluminum provides a higher temperature of combustion products and thus increased velocity of gas flow from a rocket motor, resulting in a greater specific impulse. It also raises the density of the grain and very importantly alleviates certain combustion instabilities by quenching the acoustic resonant oscillations forming in rocket motors, which would otherwise lead to structural damage of the motors during flight. A standard rocket propellant for aerospace applications consists of about 70% ammonium perchlorate crystalline oxidizer, 16–20% solid aluminum powder held in a 10–14% binder matrix consisting of an organic polymer and a plasticizer. Typically the aluminum is used in a spherical form with particle sizes of 7, 15, or 30 μm (Type I, II, III).

In the literature the combustion of aluminum particles in propellants is described extensively and reveals that the particle ignition prevalently occurs or is localized in the gaseous burning propellant flame [2,3], at times on the propellant surface or burning front, and is accompanied by the melting and often agglomeration of the aluminum on the propellant surface itself. Questions were raised in the literature [2,3] as to whether the agglomeration may be impeding the combustion process and slowing the burning velocity, whether combustion of the metallic particles may be incomplete in part due to the oxide coating present on the aluminum surface, and whether condensed oxide combustion products or slag formation may result in a reduction of motor efficiency. Nanoaluminum was thus investigated as a potential solution for reducing agglomeration and increasing ignition efficiency.

Evidence of increased solid rocket propellant burn rates by the use of nanoaluminum is reported in the literature [4]. The influence of nanoparticles of aluminum on the propellant flame was examined by high-speed photography and confirmed to produce a very homogeneous combustion throughout the flame [5]. Differential Scanning Calorimetry (DSC) data on certain ALEX nanoaluminum lots revealed the presence of lower temperature exotherms, which were attributed to the phenomenon of ''structural bond release energy'' [6], and Thermo-Gravimetric Analysis (TGA) data on the nanoaluminum show a weight change starting at $-515°C$ (below the melting point of aluminum of 660°C and ignition temperature for aluminum, which is above 2000°C). The reported ''extra'' heat produced and detected by DSC was considered as arising from the release of bonds in the crystal structure, where strain was believed to have accumulated during the manufacturing process. The extra ΔH produced by the nanoaluminum was considered as an added potential beneficial property of the nanomaterial.

In addition the nanoaluminum consists of a very fine ''dust'', which carries intrinsic toxicology, fire, and explosion hazards. Thus aluminum is generally considered nontoxic, except when it is inhaled in the form of dust. It is a hazardous material, as it is flammable and may cause fires and dust

Downloaded At: 13:47 16 January 2011

explosions, especially in the ultrafine form. Aluminum dust ignites with severity at 650°C [7]. The accumulated static charges are the basis for ''dust explosions'' and become important when dealing with nanopowders of aluminum [8]. Safe solutions to the hazard properties can be easily implemented by ensuring continuous electrostatic neutrality or discharge at each step of the manufacturing process unless ''dust explosion'' phenomena might be desired, for which different solutions can be implemented depending on the application.

A deep understanding of the physio-chemical properties of aluminum is important in learning how to exploit its full potential in different applications better. A ''micro-scale'' study of the physio-chemical phenomena in nanoaluminum is described in this paper. A follow-up paper describes the observed ''nanovision'' in depth. Such developments include an in-depth atomic-scale understanding of the materials, the properties of which display at the bulk level.

Downloaded At: 13:47 16 January 2011

Observations and Results

Chemical Analysis

Figure 1 is a photograph of the nanoaluminum examined and a sample of standard ultrafine ''flaked'' aluminum. The manufacturing technologies for the production of the two materials are different. As can be seen from the photograph, the nanoaluminum appears as a black powder. In contrast the standard ultrafine aluminum has the lustrous silvery color typical of aluminum. The difference in coloration is striking. Micron-sized aluminum used in propellant formulations appears as a whitish-gray powder. The white color comes from a surface layer of aluminum oxide covering the lustrous light-gray aluminum. Note that different sources of nanoaluminum (and other metallic nanopowders) have a similar appearance.

The dark coloration indicates that the material is absorbing the optical radiation. The black coloration of the nanoaluminum led to the question of whether some impurity/ies present in the nanoaluminum could be rendering the material black, and if so

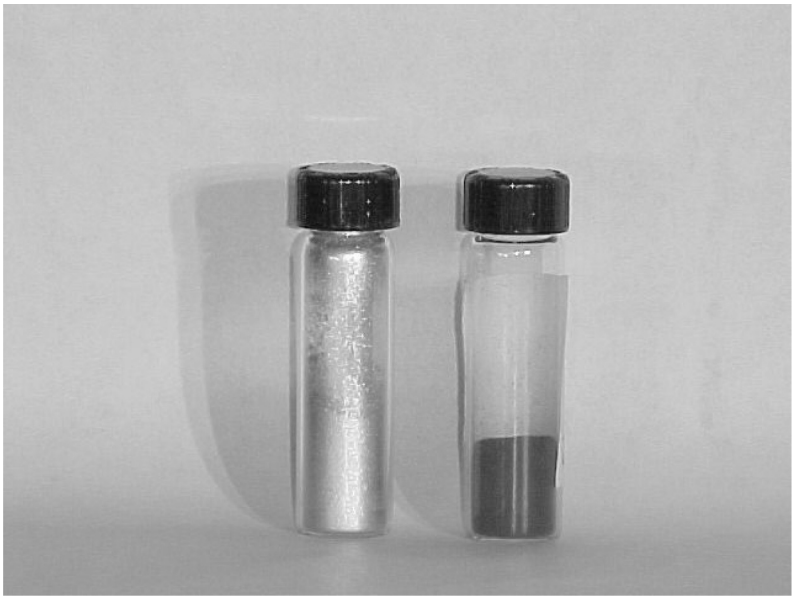

Figure 1. "Standard" ultrafine aluminum and "nanoaluminum" compared.

Downloaded At: 13:47 16 January 2011

what their effect would be on the combustion properties of the material. Chemical analysis of the material was thus undertaken. Potential candidate impurities were considered as elements present in the original raw aluminum from which the nanopowder is made, elements from the bulk aluminum ore, and/or black-colored impurities, which may have been picked up during the manufacturing process.

Wavelength Dispersion Spectroscopy (WDS) was performed using a JEOL electron microscope Model JXA8900R WD microprobe analyzer. The results are given in Table 1. As can be seen from the table, no major impurities were detected with this technique, except for oxygen, which is present on the surface of the aluminum in the form of an oxide. WDS results from rough surfaces, characteristic of the granular nanopowder, have an uncertainty of up to 5–10%.

Table 1
WDS data for the nanoaluminum

Element	Weight	Atomic percentage
o	20.7%	30.6%
Al	79.3	69.4

Prompt Gamma neutron Activation Analysis (PGAA) was performed on the samples to detect impurities that could not be revealed by WDS. In particular WDS cannot be used to detect hydrogen. Boron can be detected only at relatively high concentrations. PGAA, on the other hand, has a particularly high sensitivity for hydrogen and boron, but a very low sensitivity for oxygen and a variable sensitivity range for other elements.

The PGAA spectrometer used was located at the Materials Science and Engineering Laboratory of the NIST Center for Neutron Research in Gaithersburg, Maryland, and uses neutron guide NG-7. The maximum beam area is 50 mm × 50 mm. The apparatus is controlled through an Ethernet-based ADC-MCA workstation. The sample is continuously irradiated with a beam of neutrons. The constituent elements of the sample absorb some of these neutrons and emit prompt gamma rays that are measured with a high-resolution gamma-ray spectrometer. The energies of these gamma rays identify the neutron-capturing elements, while the intensities of the peaks at these energies reveal their concentration.

Nanoaluminum and ultrafine aluminum samples were inserted in polytetrafluoroethylene or Teflon^{TM} bags with a small hole at the top for the vacuum, mounted in the chamber and evacuated with a mechanical vacuum pump. The vacuum eliminates the possibility of detecting atmospheric elements such as nitrogen. The samples were analyzed before and after drying and were dried by placing them in a vacuum oven at 100°C for some time, followed by 90°C for 12 hr. Figure 2 shows a typical PGAA curve obtained for the nanoaluminum, and Table 2 gives the PGAA data.

Downloaded At: 13:47 16 January 2011

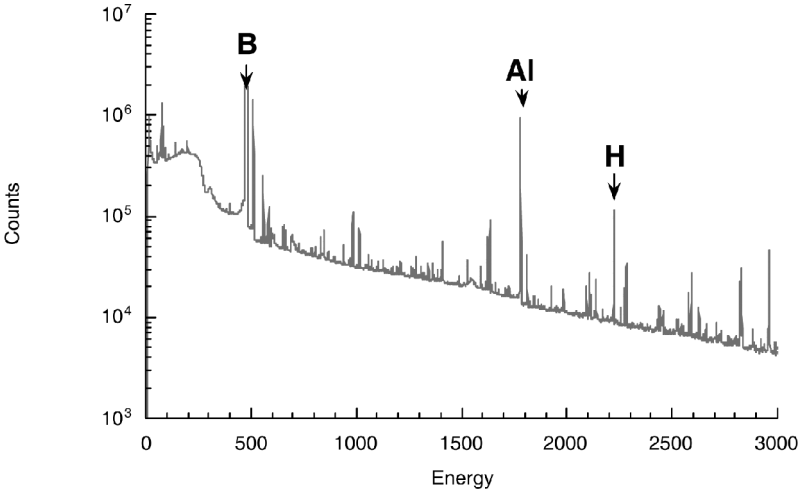

Figure 2. PGAA curve evidencing the presence of boron (B) and hydrogen (H) impurities in the nanoparticles of aluminum (Al).

Downloaded At: 13:47 16 January 2011

As can be seen from the data, boron and hydrogen impurities are present in the nanoaluminum. There was loss of some hydrogen (H) upon baking but not all. This indicates that water was trapped in the porous oxide surface. The remaining hydrogen (H) may be present in the form of aluminum hydroxide. Crystalline boron is jet-black in color. It thus appears that the black coloration of the nanoaluminum may be due to nanoscopic areas of crystalline boron possibly concentrated within the surface oxide layer on the particles. The boron impurity may have been picked up during the nanoaluminum manufacturing process since it is not typically present in the aluminum ore and raw aluminum.

Typically powdered samples of boron appear as dark gray rather than a black powder, due to the fact that it mostly consists of amorphous rather than crystalline boron. The PGAA data reveal about 0.0016 moles of boron for every 1.0 mole of aluminum. This was found in too low a concentration to be picked up by X-ray diffraction. The boron impurity detected

Downloaded At: 13:47 16 January 2011

Table 2
PGAA-results

Sample	Impurity	mg of impurity/mg of Al	Moles of impurity/moles Al
Nanoaluminum before drying	Boron	$6.55 \times 10^{-4} \pm 6.19039 \times 10^{-6}$	$1.546 \times 10^{-3} \pm 1.46064 \times 10^{-5}$
	Hydrogen	$4.67 \times 10^{-3} \pm 1.7895 \times 10^{-5}$	$1.2522 \times 10^{-1} \pm 4.79 \times 10^{-4}$
Flaked aluminum before drying	Boron	$1.351 \times 10^{-5} \pm 1.27864 \times 10^{-7}$	$3.373 \times 10^{-5} \pm 3.19127 \times 10^{-7}$
	Hydrogen	$3.56 \times 10^{-3} \pm 5.3798 \times 10^{-6}$	$9.519 \times 10^{-2} \pm 1.44 \times 10^{-4}$
Nanoaluminum after drying	Boron	$6.388 \times 10^{-4} \pm 6.06944 \times 10^{-6}$	$1.594 \times 10^{-3} \pm 1.51483 \times 10^{-5}$
	Hydrogen	$2.82 \times 10^{-3} \pm 4.6139 \times 10^{-3}$	$7.543 \times 10^{-2} \pm 1.235 \times 10^{-3}$
Flaked aluminum after drying	Boron	$1.358 \times 10^{-5} \pm 1.28373 \times 10^{-7}$	$3.389 \times 10^{-5} \pm 3.20398 \times 10^{-7}$
	Hydrogen	$2.51 \times 10^{-3} \pm 3.9975 \times 10^{-6}$	$6.726 \times 10^{-2} \pm 1.07 \times 10^{-4}$

in the flaked material is believed to originate as a contamination from some nanoaluminum left in the PGAA chamber and can thus be ignored. Measurements of the nanoaluminum were taken every time the day prior to those of the flaked aluminum. Through the small hole in the Teflon^{TM} bag and under vacuum, some of the nanopowder was found to be released into the PGAA chamber and remain as background contamination, which disappeared only after cleaning the chamber, but appears to be present in each of the flaked aluminum measurements.

After the vacuum drying of the nanoaluminum the PGAA data show that the molar ratio of hydrogen/aluminum lost by the nanoaluminum is 0.04979 compared to 0.02793 for the ''flaked'' aluminum, or about twice as much water was absorbed by the nanoaluminum. In fact, after dehydration the level of hydrogen (H) is similar in both samples, that is, $\sim$0.07 moles of hydrogen versus aluminum. This indicates that the surface oxide in the nanoaluminum is more porous than in the ''flaked'' aluminum. In fact, had it been a purely surface area effect, one would expect more water on the flaked sample because there is more surface area per unit mass of material compared to the spherical nanoparticles, which is not observed. This further confirms that the surface oxide on the spherical nanoaluminum particles has a greater porosity.

In addition X-ray Photoelectron Spectroscopy data on the nanoaluminum [9] report the finding of the following impurities on the surface of the particles: iron, copper, potassium (and nitrogen for ALEX). These impurities agree with the ones present in the raw aluminum material used for the manufacture. TGA data on the nanoaluminum show a weight change starting at 515°C (below the melting point of aluminum of 660°C) and low-temperature DSC exotherms [6]. These observations were previously attributed to the phenomenon of ''structural bond release energy.'' The revelation of impurities, especially light-element impurities such as hydrogen (and nitrogen in ALEX), and fuel ingredients such as boron provide evidence for the fact that the impurities may in fact be inducing auto-catalytic reactions, lowering the temperature of ignition for the nanoaluminum. In fact, the ALEX material, which appears to have a

Downloaded At: 13:47 16 January 2011

relatively higher content and "variety" of impurities, shows greater evidence of lower DSC temperature exotherms [6].

High-resolution Microscopy

The morphology of the nanoaluminum and the ultrafine "flaked" aluminum was examined by atomic force microscopy and high-resolution transmission electron microscopy. The uniform sphericity of the nanoaluminum particles is evidenced by Atomic Force Microscopy (AFM) micrographs, as shown in Figure 3.

AFM was performed at the Army Research Laboratory with a VEECO Metrology (formerly Digital Instruments) Dimension 3100 atomic force microscope with Nanoscope Illa controller and Phase-DO1 external electronics in tapping mode with silicon TESPW probes. It is apparent from the AFM micrographs that the nanoaluminum has a very spherical structure and narrow particle size distribution, with nominal particle sizes ranging between 60 and 70 nm.

Downloaded At: 13:47 16 January 2011

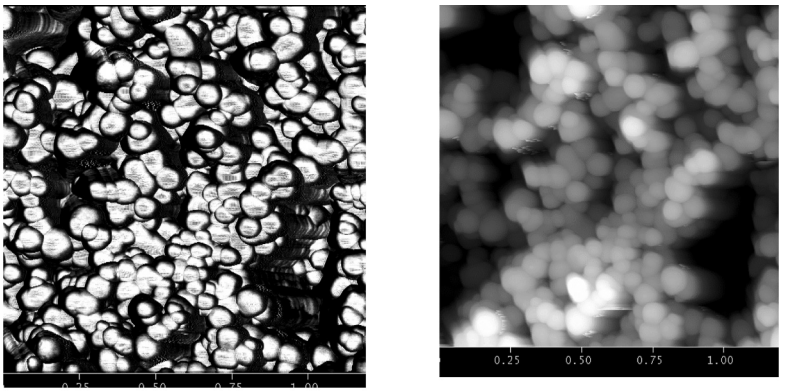

(a) (b)

Figure 3. Atomic force micrographs of nano-Al particles ($1.25\,\mu m^2$ area), with a uniform, spherical ($\sim$60–70 nm) morphology: (a) phase image, (b) height image.

The samples were also analyzed with a high-resolution electron microscope Japanese Electron Optics Limited Model 1200 EX-2 with the microscope set for the high-resolution transmission mode. Figure 4 shows a typical high-resolution transmission electron micrograph (NREM) of the nanoaluminum particles. A detailed study of the particle morphology in the micrographs

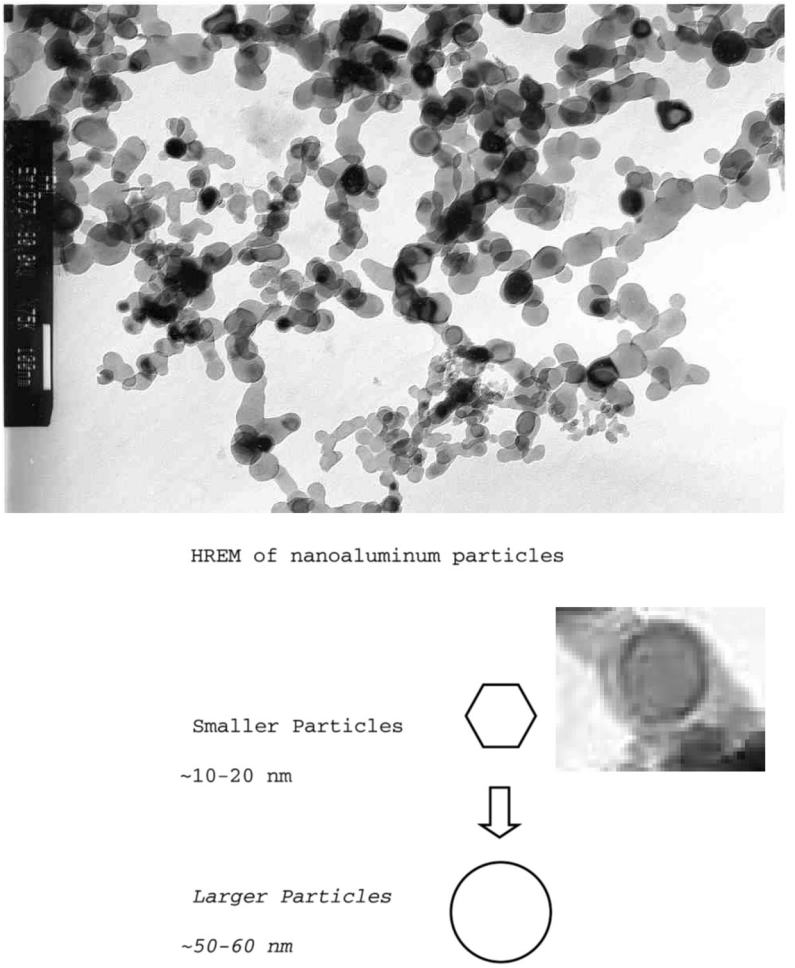

Figure 4. HREM of nanoaluminum.

Downloaded At: 13:47 16 January 2011

shows that the smallest particles are crystallographic in shape and become more spherical as the particle size increases. The crystallographic shape of the smaller particles is evidence for the formation of metal clusters by atomic aggregation in an inert atmosphere. A ''halo'' is visible around the particles. It is about 2.5 nm thick and consists of the oxide, or hydroxide surface, as evidenced by PGAA and WDS, and verified by electron microscopy of the sample at even higher resolutions as described in a follow-up paper.

In comparison with nanoaluminum, ultra-fine ''flaked'' Al particles are much larger (see Figure 5 for which the 1 μm size area shows only a section of a single particle). The ''nano-granular'' structure of the flaked aluminum is very clearly revealed by the atomic force microscope. The particle itself seems to have many nanoscale subunits that have fused together.

An HREM of the standard ultrafine aluminum is shown in Figure 6. As can be seen from the micrograph, the standard aluminum appears in flaked form where the length/width of the flakes is on the order of a few microns to submicrons in dimen-

Downloaded At: 13:47 16 January 2011

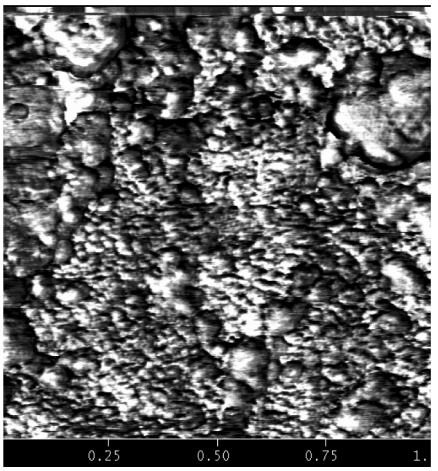

Figure 5. Atomic force micrographs (1.25 μm^2 area) of ultrafine Al flakes, showing that although submicron structures are present, they are fused together onto a much larger crystal.

Figure 6. HREM of standard ultrafine aluminum.

Downloaded At: 13:47 16 January 2011

sion and the thickness is a few nanometers. Further examination of the flakes shows that they have a granular structure where the grains are a few 100 nm in length/width down to 5–10 nm and with a thickness of 5–10 nm in agreement with the atomic force micrographs.

X-ray Diffraction

An X-ray diffraction scattering experiment was performed on the sample of nanoaluminum. X-ray powder diffraction (XRD) patterns were recorded using a Bruker D2 Discover X-ray Powder Diffractometer (CuKα radiation) and analyzed with

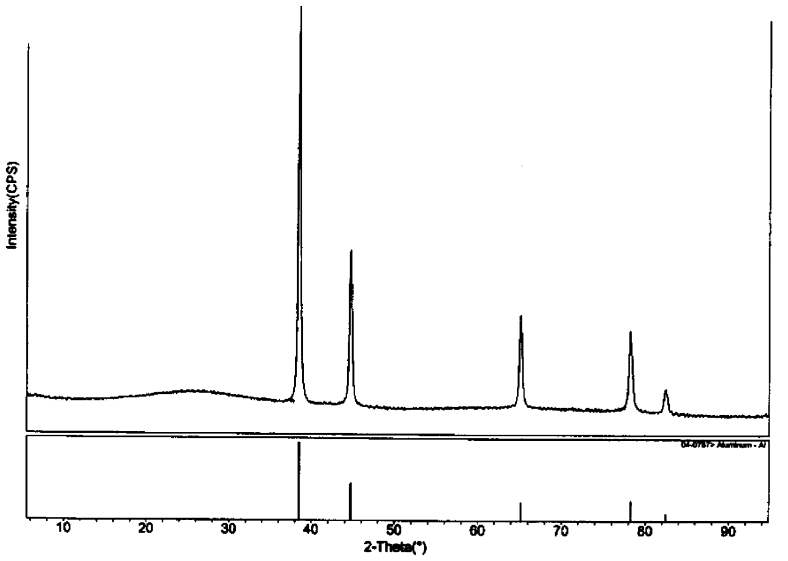

Figure 7. XRD scattering measurements for nanoaluminum and 100% Al compared.

Downloaded At: 13:47 16 January 2011

an MDI software analysis system. The X-ray scattering plot obtained is shown in Figure 7. The corresponding peaks for pure 100% Al are shown on the graph. A perfect correlation can be seen. The result indicates that the nanoaluminum sample appears not to contain any other large crystalline components or that the aluminum oxide or hydroxide is present in a prevalently amorphous state.

Table 3 gives the XRD data for the nanoaluminum and standard aluminum compared. The breadth of the X-ray peaks, given as $\sigma(Q)$, is inversely proportional to the size of the particles. Thus the sample used as "standard" shows greater peak broadening, indicative of smaller particle sizes. This is in agreement with the high-resolution microscopy where the flakes were found to consist of nanoscopic granular areas about 5–10 nm in dimension as compared with particles 60–70 nm in diameter for the nanoaluminum. Furthermore the X-ray diffraction data show accurate constants for the aluminum lattice, indicative of no residual strain in the particles and in agreement

Table 3
X-ray diffraction data on the standard aluminum and nanoaluminum compared

Sample	H, K, L	σ (Q)	a (Å)
Al flaked	1, 1, 1	0.0255 ± 0.0002	4.0267 ± 0.0002
Al nanopowder	1, 1, 1	0.0255 ± 0.0002	3.9573 ± 0.0002
Al flaked	2, 0, 0	0.0295 ± 0.0002	4.0344 ± 0.0002
Al nanopowder	2, 0, 0	0.0259 ± 0.0002	3.9835 ± 0.0002
Al flaked	2, 2, 0	0.0288 ± 0.0004	4.0497 ± 0.0003
Al nanopowder	2, 2, 0	0.0243 ± 0.0004	4.0519 ± 0.0002
Al flaked	3, 1, 1	0.0292 ± 0.0004	4.0503 ± 0.0003
Al nanopowder	3, 1, 1	0.0247 ± 0.0002	4.0780 ± 0.0001

with the lattice constant for the face cubic-centered lattice of aluminum. This is further indication of the absence of stored strain in the crystal lattice, which is mentioned in the literature [6] as the source for "structural bond release energy."

Downloaded At: 13:47 16 January 2011

Electrostatic Measurements

Finally, the residue electrostatic charges present on the nanoparticles of aluminum were measured with a standard portable electrostatic meter. The portable static meter used consisted of a surface DC volt meter built by Alphalab Inc., Salt Lake City, Utah. Table 4 shows the measured results. The electrostatic

Table 4
Electrostatic measurements on nanoaluminum and standard aluminum compared

Sample label[a]	Volts at 1″	Volts/mm
Nanoaluminum	30	1
Flaked aluminum	8	0.3

[a]Temperature: 19.5°C, Humidity: 41% RH.

meter reveals the presence of some charge, especially on the nanoaluminum sample. In fact, the nanoaluminum powder, which appears to have a higher static component, tended to agglomerate and stick to the surfaces, whereas the standard aluminum ran very smoothly when poured out of a beaker. As an indication, the field strength at ground under a lightning storm varies in strength and polarity and is often 10 kV/m or 10 V/mm or more.

The accumulated charge can form during the production, mixing, pouring, and handling of the material and can be reduced or eliminated by continuous discharging processes and/or humidity. This is important as various reported inadvertent ignitions took place even for cases where the nanoaluminum was considered to be ''passivated'' by a thick oxide ''coating.'' The ''coating'' per se can reduce the pyrophoric reaction but does not affect an inadvertent dust explosion due to any accumulated electrostatics.

Downloaded At: 13:47 16 January 2011

Discussion

Summary of the Observations

The morphologies, size, and particle distributions for nanoaluminum and flaked ultrafine aluminum samples have been measured by AFM and high-resolution transmission electron microscopy. The smaller nanoaluminum particles (~10–20 nm) are crystallographic in shape, in agreement with the formation of metal clusters by atomic aggregation in an inert atmosphere. This phenomenon is explained in Figure 8, where for smaller particles, crystal facets become more evident. The oxide on the nanoaluminum appears to be amorphous and more porous than that on the flaked aluminum, absorbing approximately two times more atmospheric humidity. X-ray diffraction data show a pristine aluminum crystalline lattice with an accurate lattice constant evidencing no residual strain in the particles.

Impurities of boron, hydrogen, and water were detected in the nanoaluminum. The boron (B) impurity appears to be in the form of nanoscopic crystalline areas of the coating, rendering

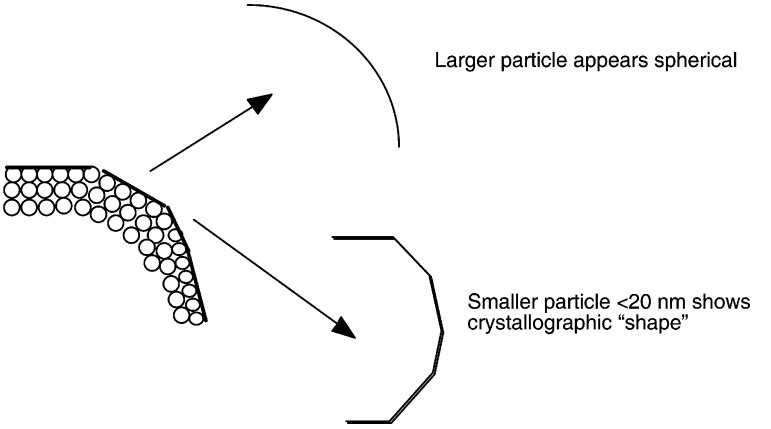

Figure 8. Morphology of nanoparticles as a function of particle size.

Downloaded At: 13:47 16 January 2011

the material black. The presence of the impurities is related to the possibility for auto-catalytic reactions, otherwise attributed to "structural bond release energy," especially where light-element impurities are involved. The nitrogen detected in the ALEX nanoaluminum may be in the form of aluminum nitride in the same way that aluminum oxide is formed. Oxidation of aluminum nitride in air will occur at temperatures above 700°C. Additionally when one considers that nitrogen is one of the main constituent elements of explosives, the nitrogen present within the nanoaluminum may potentially be incorporated in such a way as to make the material "part-explosive" by triggering the appropriate physio-chemical reaction. The incorporation of light-element-tailored impurities during the manufacture may provide for new improved forms of nanoaluminum by "atomic-scale design." The data should also be studied to understand and optimize the process of aging under various conditions.

An oxide surface, 2.5 nm in thickness for nanoparticles with a diameter of 60 nm, consists of a molar ratio of $\sim$0.133 of oxygen versus aluminum. This is equivalent to or close to the

molar ratio for hydrogen (H) in the nanoaluminum before drying, which is ∼0.13 and might indicate that the oxide has almost entirely converted to aluminum hydroxide. However, the fact that 0.07 molar ratio of hydrogen is released in the form of water shows that about half of the hydrogen was residing in the form of water molecules and the rest in the form of hydroxide. Thus for every one out of two oxygen atoms (0.07/0.133) a hydrogen atom was bonded with an oxygen atom to form a hydroxyl group, and for the remaining oxygen atoms one water molecule (H_2O) was hydrogen bonded to two oxygen atoms in the aluminum oxide, giving a ratio of 1:1 for hydrogen atoms versus oxygen atoms overall.

Now, 2.5 nm of oxide consists of about six molecular layers (or six unit cells, where 4.05 Å is the unit cell lattice spacing for the face-centered cubic structure of aluminum). After drying, it is most likely that the hydroxide resides in the bottom-most molecular layers as depicted in Figure 9, the water having resided in the topmost molecular layers. In the case of the flaked aluminum only 0.02 molar ratio of hydrogen resides in water molecules. This gives an oxide structure as shown in Figure 9, where it can be seen that the water molecules have permeated up to only ∼3–4 molecular layers of oxide compared to ∼6 for the nanoaluminum, further proving the greater porosity of the oxide in the nanoaluminum.

The boron is present at the level of 0.0016 moles versus 1.0 mole of aluminum. This consists of about 2 atomic% of boron compared to aluminum in the surface oxide and proves that the boron (B) is possibly concentrated in the outermost molecular layer, where the boron content would increase to ∼12 atomic%. It is also of interest to consider that crystalline boron reacts or ignites differently from amorphous boron.

Finally, static charges have been measured and confirmed on the nanoaluminum and agree with the reported inadvertent ignitions that have occurred in the handling of nanoaluminum. This can easily be resolved by ensuring continuous discharge through proper grounding/earthing of any accumulated charges during the manufacturing, mixing, or pouring processes where nanoaluminum is involved unless ‘‘dust explosion’’ phenomena

Downloaded At: 13:47 16 January 2011

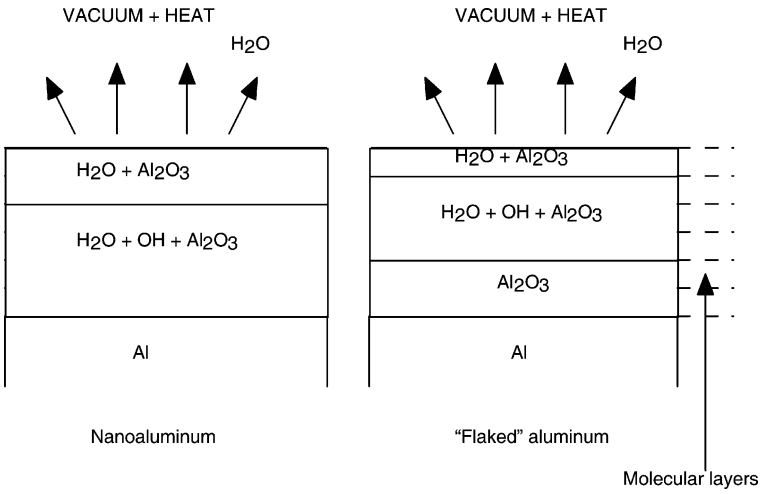

Figure 9. Surface oxide in nanoaluminum and "flaked" aluminum.

Downloaded At: 13:47 16 January 2011

might be desired, for which different solutions can be implemented depending on the application.

Summary of Physio-chemical Processes

By examination of the physio-chemical properties of aluminum some of the questions related to the use of nanoaluminum in propellant formulations, as described in the introduction, can be addressed. Figure 10 shows a summary of the microscale physio-chemical effects that appear to occur in the aluminum nanoparticles during the propellant surface combustion. Figure 11 shows the physio-chemical effects occurring in the nanoparticles of aluminum leading up to their ignition in the propellant flame.

Figure 10 depicts the combustion of the propellant, which occurs at several hundreds °C. The aluminum particles thus increase in temperature from ambient to their melting point. The aluminum metal acts as a heat sink in rapidly absorbing heat (and releasing it if the surrounding environment is at a

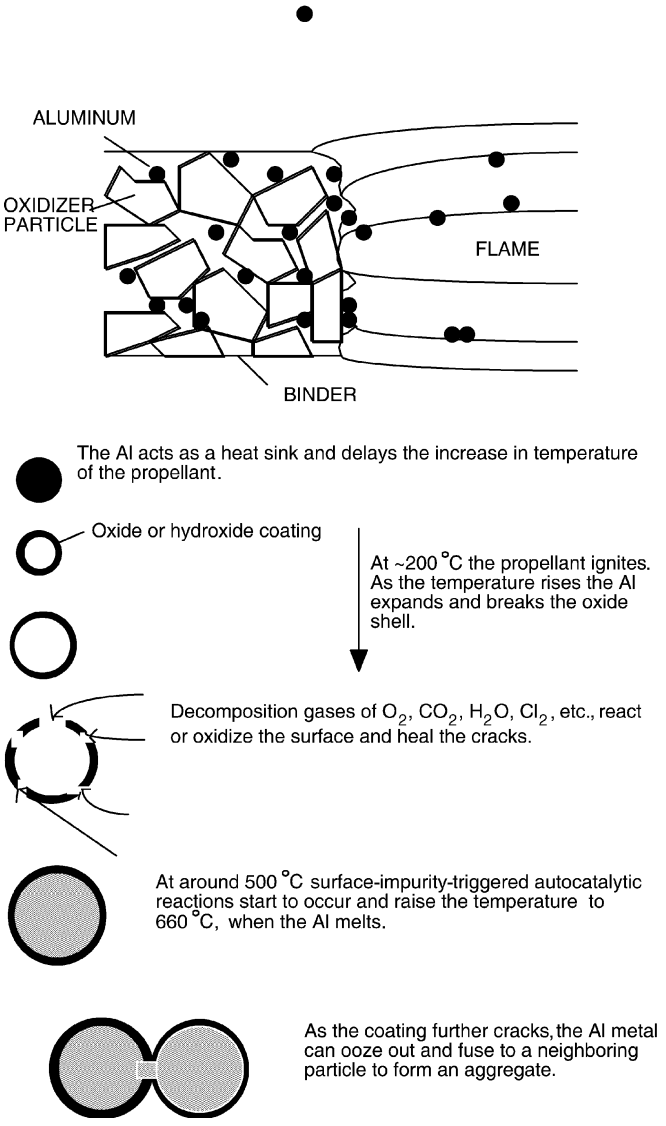

Figure 10. Physio-chemical phenomena in nanoparticles of aluminum.

Downloaded At: 13:47 16 January 2011

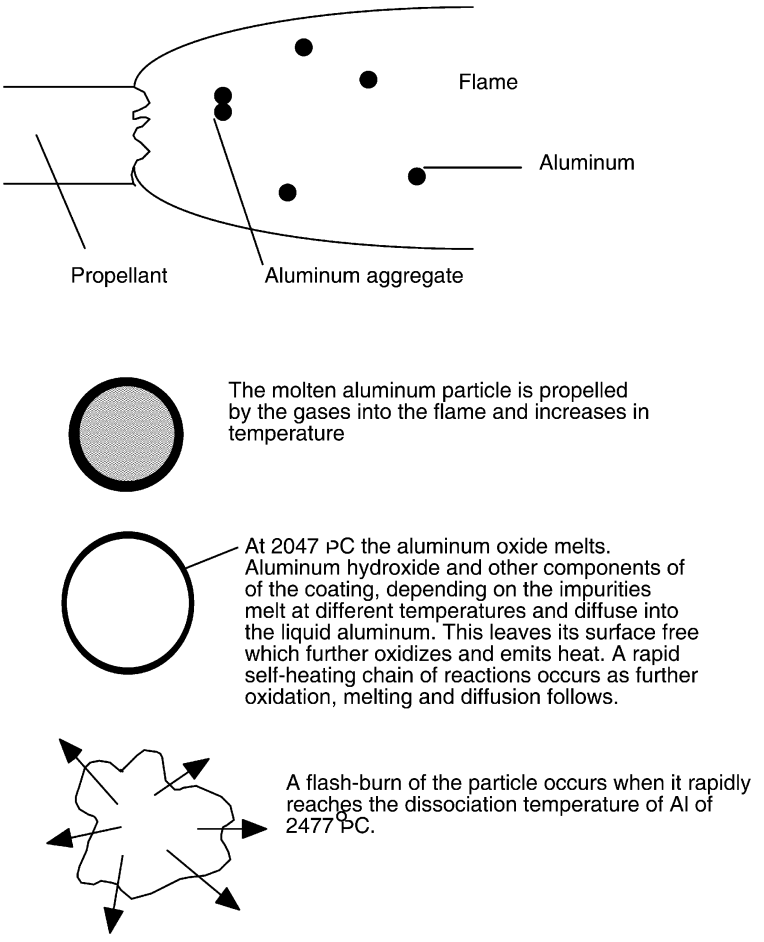

Figure 11. Ignition of the nanoparticles in the flame.

lower temperature) and delays the surface increase in temperature of the propellant. The nanoaluminum particles act as less of a heat sink compared to micron-sized particles, thus allowing for a quicker propellant burn. As the temperature of the aluminum particles increase, prior to their melting point, the particles expand, eventually breaking the oxide coating. Decomposition gases of O_2, H_2O, CO_2, Cl_2 etc., react with the exposed

Downloaded At: 13:47 16 January 2011

aluminum in the oxide cracks and ''heal'' the cracks as reported in the literature [10].

For the nanoaluminum, at around 500°C impurity-triggered auto-catalytic reactions occur and rapidly raise the temperature to 660°C, at which point the aluminum also melts. As the coating further cracks, the molten aluminum oozes out and fuses with the molten aluminum trickling out from the neighboring particle crevices, thus forming aggregates. Finally, as can be seen in Figure 10, the forces of gas flow pull the molten aluminum aggregates or single particles into the flame stream, where the temperature of the particles further increases.

As shown in Figure 11, the increase in temperature of the molten aluminum particles in the gaseous stream leads to their ignition. The boiling point of aluminum is 2518°C, and the dissociation temperature is 2477°C. The fact that the dissociation temperature is lower than the boiling point is indicative of the fact that heat is absorbed during the dissociation process to separate the atoms. This absorption of heat lowers the overall temperature.

The liquid aluminum is ''contaminated'' with liquid aluminum oxide, hydroxide, nitrides, chlorides, etc., and impurities residing in the aluminum surface, either from the ''healing'' of the coating cracks or from impurities already present in the nanoaluminum. The melting point, for example, for aluminum oxide is 2047°C. The impurities further reduce the boiling point of aluminum, and as they dissolve in the liquid aluminum droplet, surface oxidation of the droplet becomes accelerated since the surface of the aluminum cannot stay unoxidized and continues to draw oxygen to its surface. As the oxidation takes place, further heat is released, the molten oxide enters the droplet, and more surface oxidation takes place, until the process accelerates to a point where the aluminum temperature has rapidly increased to the dissociation point, and the droplet dissociates with a sudden flash. Oxidation itself is thus an autocatalytic process, and the fact that an oxide surface is already present on the particles appears to catalyze the oxidation rather than impede it, as assumed in some of the literature [2,3]. This has been observed in high-speed photography [2]

Downloaded At: 13:47 16 January 2011

where the whole process can take place from 5 to 50 ms, and there is typically a gaseous plume surrounding the incandescent oxidizing aluminum particle. The effect of the oxide, hydroxide, and other impurities may thus in fact be one of "catalytic" action as well as "lowering" the temperature for aluminum ignition.

Acknowledgments

The authors wish to thank Dr. Rick Paul for helping in the analysis of the NIST PGAA data. Dr. Mary Campbell of LANL is thanked for discussions of the TGA data. The CAD/PAD Dept., NAVSEA-IH, is thanked for the nanoaluminum samples and for support of some of the investigative work on nanoaluminum. Dr. Brad Forch is thanked for his valuable encouragement and guidance throughout. Dr. John Kolts and DTRA is further thanked for support under the Advanced Energetics Research Program FY02-WMR-044. ONR is thanked for support of some of the fundamental work, and ARL is thanked for collaborative work on the project as a whole. Special gratitude goes to Dr. Richard Miller for having paved the way to progress in the science of energetic materials.

Downloaded At: 13:47 16 January 2011

References

[1] Federoff, B. T., ed. 1960. "Encyclopedia of Explosives and Related Items," Picatinny Arsenal, vol. 1, p. A142.

[2] Zarko, V. E. 1998. Chapter 10. In *Modelling and Performance Prediction in Rockets and Guns*, ed. S. R. Chakravarthy and S. Krishnan, p. 301. City: Allied Publishers.

[3] Price, E. W. 1984. Chapter 9. In *Fundamentals of Solid-Propellant Combustion*, ed. K. Kuo and M. Summerfield. p. 479. *Progress in Astronautics and Aeronautics*, vol. 90.

[4] Fisher, M. and M. Sharp. 2002. "Solid Rocket Propellants for Improved IM Response: Recent Activities in the NIMIC Nations," AVT (Applied Vehicle Technology Panel) RTO-NATO Meeting on "Advances in Rocket Performance Life and Disposal," Aalborg, Denmark, 23–27 September.

[5] Chan, M. L. 2000. "Properties of ADN Propellants." International Meeting on Special Topics in Chemical Propulsion. In *Combustion of Energetic Materials*.City: Begell House.
[6] Hlaveck, V. 2002. "Energy Storage in and Combustion of Ultrafine Powders." In *Proceedings from DIA New Materials III Symposium*, 2–4 April.
[7] *Marks' Standard Handbook for Mechanical Engineers*. Edited by T. Baumeister, E. A. Avallone, and T. Baumeister, 8th ed., pp. 7–29. New York, McGraw-Hill.
[8] Ramaswamy, A. L. 2000. "Improving the Sensitivity of Metastable Intermolecular Composite (MIC)." CAD/PAD NSWC-IH Report. July.
[9] Hooton, I. 2002. "Nanopowders: Characterization Studies." In *Proceedings of the DIA New Materials III Symposium*, 2–4 April.
[10] Crump, J. E., J. L. Prentice, and K. J. Kraeutle. 1969. *Combustion Science and Technology*, 1: 205.

Downloaded At: 13:47 16 January 2011